ChemPubSoc Europe

DOI: 10.1002/cctc.201901112

CHEMCATCHEM Full Papers

Suzuki-Miyaura Cross-Coupling Using Plasmonic Pd-Decorated Au Nanorods as Catalyst: A Study on the Contribution of Laser Illumination

Mattheus Verkaaik,[a] Roos Grote,[a] Nicole Meulendijks,[a] Francesc Sastre,[a] Bert M. Weckhuysen,*[b] and Pascal Buskens*[a]

The interaction between plasmonic metal catalysts and visible light can be exploited to increase their catalytic activity. This activity increase results from the generation of hot charge carriers or hot surfaces, or a combination of both. We have studied the light-induced Suzuki-Miyaura cross-coupling reaction of bromobenzene and *m*-tolylboronic acid using Pd-decorated Au nanorods as plasmonic catalyst in order to assess which physical effect dominates. Comparative experiments under laser illumination and in dark were performed, demonstrating that under the experimental conditions applied in our study the catalytic activity achieved upon illumination is dominantly based on the conversion of light to heat by the plasmonic catalyst. Pd leached from the catalyst also plays a significant role in the reaction mechanism.

Introduction

Noble metal nanoparticles have an interesting property: they can be very efficient absorbers of electromagnetic radiation with wavelengths much longer than their own physical dimensions. The absorption of photons by nanoparticles leads to the formation of local surface plasmon resonance (LSPR): the collective oscillations of metal valence electrons within an individual nanoparticle.[1] The LSPR will dephase within femtoseconds, leading to excited electron-hole pairs (Landau damping), radiation damping, and damping due to electron-surface collisions.[2] These damping effects make plasmonic nanocatalysts efficient sources of heat and hot electrons, which form the fundament of plasmon catalysis and opens up ways to improve reaction speed and selectivity of chemical reactions. Especially, the harvesting of visible (VIS) and near-infrared (NIR) radiation of sunlight as a sustainable way to drive chemical reactions is intensively studied. Recently, plasmon catalysis has been demonstrated for a broad variety of important chemical reactions, ranging from steam reforming of ethanol[3] to hydrogen dissociation,[4] and reduction of CO_2 to CH_4.[5]

Catalysis by photoplasmonic nanoparticles can be attributed to hot carriers as well as to nanoparticle heating. Discriminating between the two is difficult, however. The bulk temperature of the catalyst or reaction mixture may significantly differ from the local temperature at the surface of the catalytic metal nanoparticles, where the chemical processes take place. This absolute local temperature is very challenging to measure directly and precisely on an individual nanoparticle.[6] Heat transport phenomena and reaction energetics can complicate this even further. Recently, several studies distinguishing between photochemical and photothermal contributions of plasmon-assisted catalytic systems were published.[5b,7]

A reaction that raised scientific interest in photocatalysis is the Suzuki-Miyaura cross-coupling reaction. This reaction couples an aryl halide and an aryl boronic acid to form biphenyl species over a heterogeneous Pd catalyst under relatively mild reaction conditions.[8] The reaction is widely used for the industrial synthesis of e.g. styrenes,[9] poly-olefins,[10] and biphenyls.[11] Several successful attempts were taken to incorporate a photocatalytic component into the Suzuki-Miyaura reaction, for example by the application of a semiconductive Mott-Schottky-type SiC support for the Pd nanoparticle catalyst,[12] the *in-situ* reduction of a Pd(II) complex to Pd(0) using a Ru(II) photosensitizing unit,[13] and the use of Pd nanosheets absorbing in the visible near-infrared domain.[14] The enhancement of the reaction kinetics in these plasmonic systems is widely acknowledged, but the discrimination between the catalytic contribution of Pd(0) and the photonic heating of the catalyst remains underexposed.

In this work, we have quantitatively studied the thermal and non-thermal contributions of laser illumination to the Suzuki-Miyaura cross-coupling of bromobenzene and *m*-tolylboronic acid using Pd nanoparticles decorated on plasmonic Au nanorods as catalyst (hereafter referred to as Au@Pd). This is an important reaction in the synthesis of styrenes,[9] poly-olefins,[10] and biphenyls.[11] The integration of the SCR into a plasmon-enhanced catalytic particle can be achieved by physically combining catalytic Pd nanoparticles with a plasmonic Au

[a] *M. Verkaaik, R. Grote, N. Meulendijks, Dr. F. Sastre, Prof. P. Buskens*
TNO Materials Solutions
High Tech Campus 25
Eindhoven 5656 AE (The Netherlands)
E-mail: pascal.buskens@tno.nl
[b] *Prof. B. M. Weckhuysen*
Inorganic Chemistry and Catalysis Group
Debye Institute for Nanomaterials Science
Utrecht University
Universiteitsweg 99
Utrecht 3584 CG (The Netherlands)
Fax: (+ 31) 30–251-1027
E-mail: b.m.weckhuysen@uu.nl

Supporting information for this article is available on the WWW under https://doi.org/10.1002/cctc.201901112

© 2019 Wiley-VCH Verlag GmbH & Co. KGaA, Weinheim

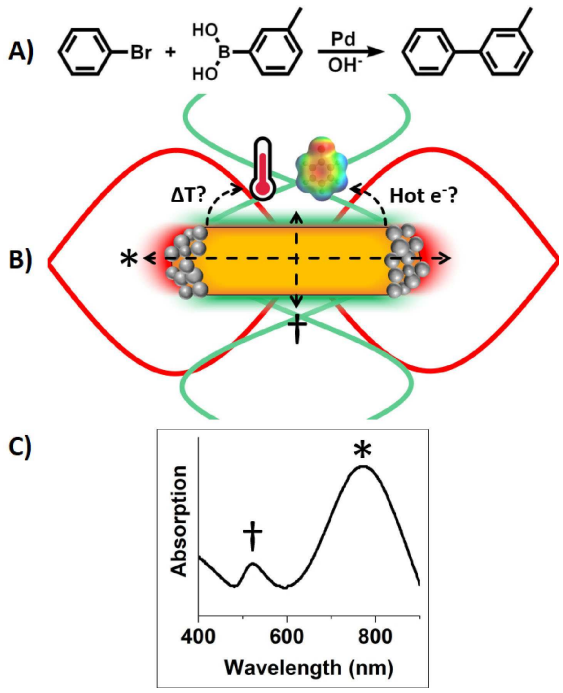

Figure 1. A) Suzuki-Miyaura cross-coupling reaction, using Pd nanoparticles as catalyst. B) Schematic of a plasmonically excited Au nanorod with Pd nanoparticle catalyst at the tips. The particle is excited by the longitudinal and transversal waves, depicted red and green, respectively. C) UV-Vis spectral positions of the longitudinal (asterisk) and transversal (dagger) of the Au@Pd nanorods with CTAB stabilizer in water.

nanorod (Figure 1B).[15] The Au nanorod is key in this plasmonically catalyzed system, because Pd nanoparticles are weakly plasmonic and only show extinction maxima in the Ultraviolet (UV) spectral region.[16] The use of Au nanorods with tunable absorption makes it possible to use the abundant NIR region of the solar emission spectrum (Figure 1C).[17]

We have studied the specific roles of plasmon-assisted chemistry and photothermal heating properties of Au@Pd nanoparticles on the bulk reaction mixture. We have comparatively studied the plasmon-assisted Suzuki-Miyaura cross-coupling reaction under laser illumination and a non-illuminated, simultaneous reference reaction to study the influences of physical parameters and reactant variations on the reaction kinetics and temperature profiles. The parallel reference reaction is continuously heated to the bulk temperature of the illuminated reaction, thereby allowing us to decouple the influences of plasmon-assisted chemistry and its associated bulk heating effects. Partial reaction orders were determined by varying catalyst and reaction concentrations, giving a clue about thermal and catalytic contributions as well.

Results and Discussion

The initial composition of all reaction mixtures consisted of bromobenzene and *m*-tolylboronic acid as reactants, NaOH as base, hexadecyltrimethylammonium bromide (CTAB) as stabilizer, and Au@Pd as plasmonically active catalyst.

For the kinetic studies, sets of two parallel reactions were performed with various parameter variations in order to quantify the roles of hot electrons and of the bulk reaction temperature. Note: all reaction temperatures reported in this manuscript are temperatures measured for bulk reaction mixtures using a thermocouple. A schematic of the used setup is shown in Figure 2A. Briefly, two parallel reactions were performed per experiment: one illuminated with an 809 nm Continuous Wave (CW) laser; the other is not illuminated but heated. This heated reaction served as a thermal reference reaction. The bulk reaction temperatures of both reactions were continuously monitored using a thermocouple submerged in the middle of the reaction mixtures. Subsequently, the temperature of the reference reaction was continuously adjusted to the temperature of the illuminated reaction using a temperature-controlled cuvette holder. This method makes it possible to distinguish between the illumination effect itself and the accompanied bulk heating of the reaction mixture.

Anticipating on the heating power of the cuvette heater on the one hand and on the laser heating power on the other is necessary to accurately match the two reaction temperatures manually: the heating power of the cuvette holder for the reference reaction is much higher than the laser heating power. We have found that it's possible to match the two temperatures manually with only a few degrees of deviation during the reaction phase with increasing temperatures.

The concentrations of the reaction mixture during the reaction were analyzed using gas chromatography (GC). With these concentrations the reaction rates were calculated in the linear sections of the graphs, using the formation of biphenyl to calculate the conversions in time. It was assumed that the breaking of the C–Br bond was the rate-determining step in this reaction.[18]

Structural and Optical Characterization of the Catalyst

Transmission Electron Microscopy (TEM) was used to validate the morphology of the particles. The particles applied in our study are rod shaped with average dimensions of 107 ± 8 nm and an average width of 49 ± 5 nm ($n = 42$), having an aspect ratio of 2.2. Energy Dispersive X-ray (EDX) images of the Au@Pd nanoparticles show a solid Au rod core, surrounded with a layer of Pd nanoparticles of approximately 5 nm in diameter. The tips of the rods show a higher concentration of Pd particles than the sides, which is in agreement with earlier publications.[15,19] This higher Pd nanoparticle concentration at the tips is desirable, since the longitudinal LSPR has a much larger absorption cross-section than its transversal counterpart, giving stronger local fields at the tips of the particle than on the sides. The plasmonic characteristics of the particles were measured with UV-VIS in diluted aqueous dispersion, as received. Absorption bands were determined at 523 nm and 772 nm,

© 2019 Wiley-VCH Verlag GmbH & Co. KGaA, Weinheim

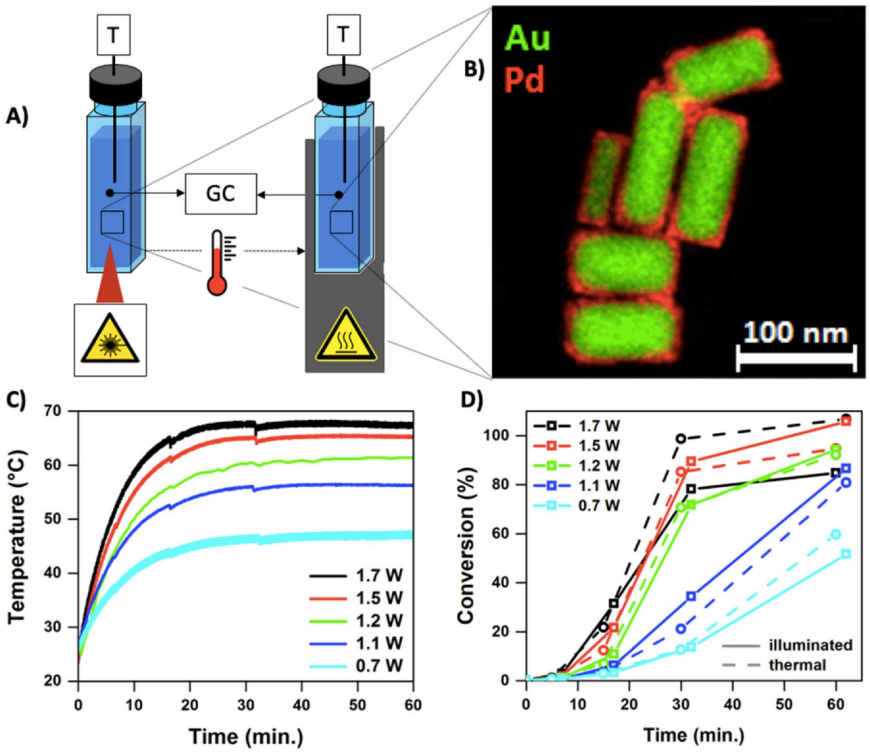

Figure 2. A) Schematic of the experimental set-up. The left cuvette is subjected to laser illumination, the right (reference) cuvette is not illuminated but continuously equated to temperature of the illuminated cuvette. T: thermocouple, GC: gas chromatograph. B) TEM-EDX images of the Au@Pd nanoparticles, showing elevated concentrations of Pd at the tips of the nanorods C) Temperature profiles of illuminated reactions with 0.7 to 1.7 W laser illumination, corresponding with 0.08 to 0.20 W/mm^2. The dips in the graphs result from reaction mixture sampling. D) Conversion plots of illuminated reactions (squares) and their thermal reference reactions (circles). Clear correlations between the illuminated and thermal reference reactions are observed, indicating a large thermal influence on the reaction kinetics, with minor contribution of photocatalytic effects.

corresponding to the transversal and longitudinal plasmon resonance, respectively. Elemental analysis of these Au@Pd nanoparticles using atomic emission spectroscopy (AES) yielded 343 μg/g Au and 214 μg/g Pd, giving an Au:Pd weight ratio of 1.60. This is qualitatively in accordance with the TEM-EDX analysis, as shown in Figure 2B.

A stable and fully dispersed catalyst during the course of the reaction is essential for obtaining useful kinetic information. Therefore, we've tested the stability of the Au@Pd nanoparticles in the reaction mixture on forehand. Some test reactions with mild illumination conditions were performed, checking for any macroscopic changes in the suspension. It was found that the acquired nanoparticle catalyst was prone to rapid agglomeration, leading to full sedimentation within 30 min. It was found that using semiconductor-grade NaOH (99.999%) instead of technical grade NaOH (98%) as base had a positive effect on the nanoparticle stability: no sedimentation was observed within 60 min of reaction.

Reproducibility of the illuminated reaction was tested by an *in triplo* experiment using standard amounts of reactants and catalyst and with 1.7 W (0.20 W/mm^2) of laser light illumination for 60 min (Figure S1). The result of this experiments demonstrates good reproducibility with a typical error of approx. 5%.

Five experiments with variable laser powers from 0.7 to 1.7 W (0.08 to 0.20 W/mm^2) were used to study the effects of resonant laser irradiation on the temperature progression and the conversion of the reaction (Figures 2C and 2D). Temperatures of the illuminated reactions immediately increase after switching on the laser, reaching a stable temperature plateau after approximately 30 min until the reaction was terminated after 60 min. The reached temperature plateaus scale with the applied laser power in each reaction. An initiation phase, characterized by an increasing slope of the conversion in time, is visible in all experiments - both under illumination as when heated. This can be explained by several phenomena.

Firstly, the viscosity of the reaction mixture is very dependent on the temperature, ranging from syrup-like at room temperature to water-like at the observed temperature plateaus. Although the viscosities of the reaction mixture as a function of temperature were not quantified, it can be assumed that mass transfer limitations play a significant role during the bulk heating in the first minutes after starting the experiments.

Secondly, the CTAB in the reaction mixture cannot be fully dissolved without elevating the temperature before starting the reaction. This results in an increase in CTAB concentration in the first phase of the reaction, with an associated increase in solubility of the bromobenzene. This might result in non-linear behavior of the reaction speed in the first phase of the reaction.

Thirdly, the temperature increase of the reaction mixture has an obvious effect on the reaction kinetics.

© 2019 Wiley-VCH Verlag GmbH & Co. KGaA, Weinheim

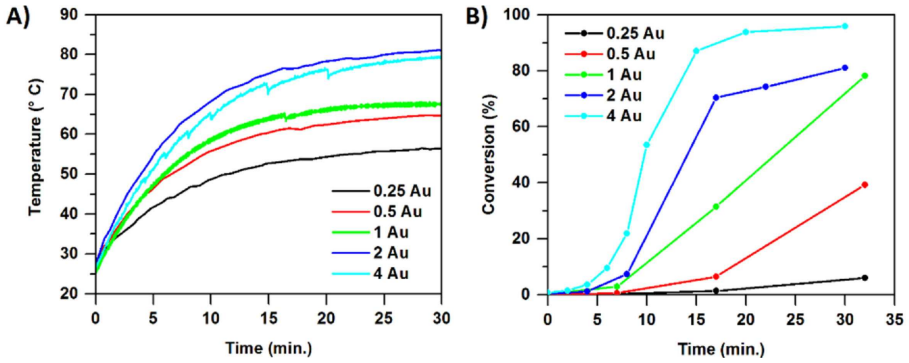

Figure 3. A) temperature plots of reactions with different amounts of Au@Pd catalyst, performed at 1.7 W (0.20 W/mm^2) laser power. B) correlations between amount of catalyst and temperature plateaus are eminent, as well as the increase in conversion speed.

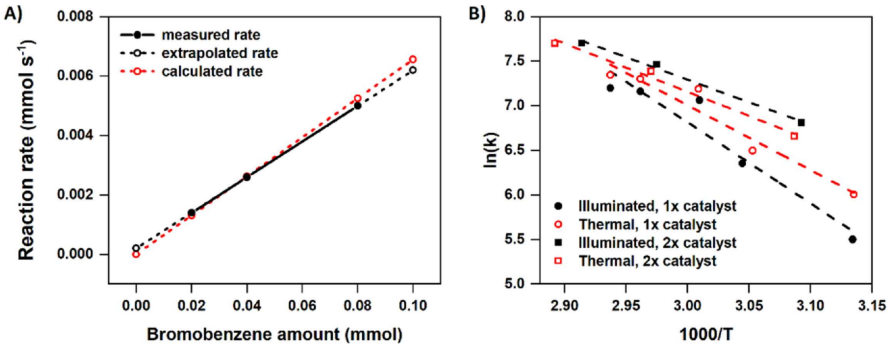

Figure 4. Effects of concentration variations in the reaction mixture. A) Reaction rates of the illuminated reaction at 1.2 W (0.14 W/mm^2) of laser power as function of bromobenzene variation. The rate in the linear area (5–30 min) was calculated. Black dots represent the measured data, red circles represent calculated values of partial first-orders of reaction in bromobenzene. The reaction was found to be first-order in bromobenzene. B) Arrhenius plots of two sets of reactions: one with a normal amount of catalyst, and a second with double amount of catalyst. Both reactions were performed with different laser intensities to obtain the values of k. These values were determined for the amount of bromobenzene per amount of nanoparticles within 25 min. The slope of the illuminated reactions and their respective thermal reference reactions are comparable, indicating a large thermal dependence of the reaction kinetics.

The influence of the amount of catalyst on the temperature progression and reaction speed was studied by changing the amount of catalyst in the reaction mixture (Figure 3). Amounts from 0.25 to 4 x the amount relative to standard amount were used, corresponding to 6.5 μg of Au and 4 μg Pd and 104 μg of Au and 64 μg Pd, respectively. A clear correlation between amount of catalyst and the temperature increase and temperature plateau was observed. The obtained conversion speeds match the temperature progressions of the reactions.

The amount of bromobenzene was varied in separate experiments to find out its partial reaction order and to check the dependence on the overall reaction speed. Three experiments with 0.25, 0.5, and 1 times the standard amount of bromobenzene were carried out at 1.2 W (0.14 W/mm^2) laser illumination (Figure 4A).

The conversion of bromobenzene as a function of the amount of Au@Pd nanoparticles was used to calculate the conversion rate. Two sets of experiments were performed: one set with varying laser powers and the normal amount of catalyst, and a second with a double amount of catalyst. The values of *k* were determined in the linear regime, after 25 min. The influence of catalyst concentration on the overall reaction rate was also studied. Two series of reactions with different laser intensities were performed: one with the normal amount; the other with a double amount of catalyst. The reaction rates were determined for the amount of bromobenzene per amount of nanoparticles within 25 min of reaction time. The results are displayed in an Arrhenius plot (Figure 4B). The Arrhenius plots from the illuminated reactions and their thermal reference reactions are similar, showing apparent activation energies of 76 (illuminated) and 61 (heated) kJ/mol for the reactions with single catalyst loading, and 42 (illuminated) and 45 (heated) kJ/mol for the reactions with double catalyst loading.

Bimetallic nanoparticles are prone to deformation and alloying upon elevated temperatures.[20] Therefore, we have studied the morphology and elemental distribution of the Au@Pd nanoparticles after exposure to laser light in the reaction mixture. Au@Pd nanoparticles were extracted from a used reaction mixture using centrifugation. TEM-EDX measurements were used to study the morphology and composition of the extracted nanoparticles. No differences between new and used Au@Pd nanoparticles were found (Figure S2).

Pd is also a common homogeneous catalyst as well as non-photonically active nanoparticle catalyst. Especially Pd is known

© 2019 Wiley-VCH Verlag GmbH & Co. KGaA, Weinheim

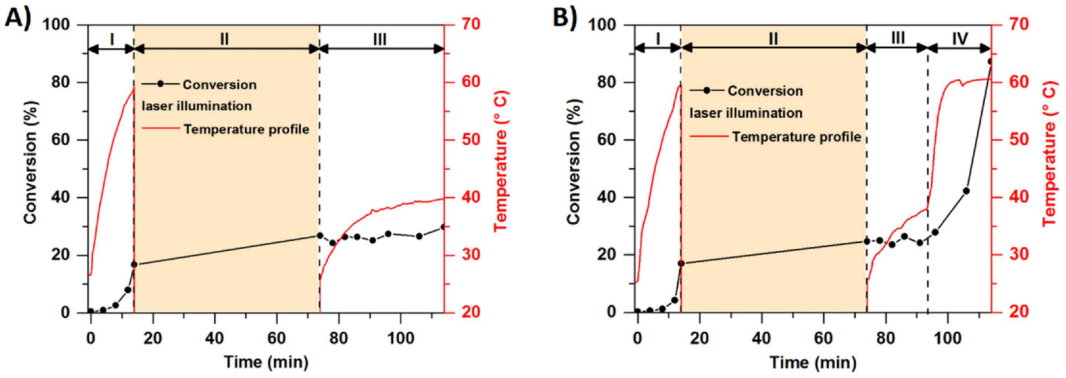

Figure 5. Hot filtration tests: (a) After 14 minutes reaction time at 1.5 W laser illumination (I), the reaction is stopped through cooling to 0 °C, and subsequently the nanorods are removed from the reaction mixture through centrifugation. After one hour (at minute 74), the rod-free supernatant was subjected to 1.5 W laser illumination, resulting in a temperature increase from 0 °C to 40 °C, which did not result in an increase in conversion (III); (b) After 14 minutes reaction time at the temperature as achieved upon illumination (60 °C, I), the reaction is stopped through cooling to 0 °C, and subsequently the nanorods are removed from the reaction mixture through centrifugation. After one hour (at minute 74) the rod-free supernatant was subjected to 1.5 W laser illumination, resulting in a temperature increase from 0 °C to 37 °C, which did not result in an increase in conversion (III). At minute 92, the reaction mixture was heated to the same temperature as obtained upon illumination of Au@Pd nanorods, i.e. 60 °C, resulting in an increase in conversion of about 20% to 90% (IV).

to leach from photocatalytic nanoparticles in basic environments, forming a highly active homogeneous Pd catalyst.[21] The influence of potentially leached Pd, which may dissociate from Au@Pd nanorods under the applied reaction conditions, was tested with two hot filtration tests (Figure 5). After 14 min, the illuminated (Figure 5a) and the thermal reactions (Figure 5b) were stopped by immersing both reaction cuvettes in ice water. The reaction mixtures were subsequently centrifuged to remove all Au@Pd nanorods. The catalytic activity of the rod-free supernatants was tested upon illumination (Figure 5a), and upon illumination and conventional heating (Figure 5b).

Before removal of the Au@Pd nanorods, the temperature of the illuminated reaction mixture increased as expected upon 1.5 W (0.17 W/mm^2) laser illumination to 60 °C (zone I in Figure 5a). This resulted in a conversion of approx. 20% in 14 minutes reaction time. After the centrifugation step in the absence of nanorods, the resulting supernatant showed no catalytic activity at a temperature of 0 °C (zone II in Figure 5a). The temperature of the illuminated rod-free reaction mixture only reached 40 °C (zone III in Figure 5a). Under these conditions, no further conversion was observed, and conversion remained at a stable level of around 20%.

The temperature of the thermal reaction, which was conventionally heated, was similar to the parent illuminated reaction during the first 14 minutes reaction time (zone I in Figure 5b). This resulted in approx. 20% conversion. After the centrifugation step in the absence of nanorods, the resulting supernatant showed no catalytic activity at a temperature of 0 °C (zone II in Figure 5b). The temperature of the illuminated rod-free reaction mixture only reached 37 °C (zone III in Figure 5b). Under these conditions, no further conversion was observed, and conversion remained at a stable level of around 20%. A subsequent temperature increase through conventional heating to 60 °C caused an immediate rise of the conversion, going from a stagnant 20% to 90% in 20 min (zone IV in Figure 5b). Based on these results, we conclude that that the plasmonic Au rods are essential for conversion of light to heat, and that catalytically active Pd species leach from the Au@Pd nanorods under the applied reaction conditions.

Conclusions

The decoupling of the photochemical and the photothermal effects of plasmonic Au@Pd nanoparticles as catalytic species in the Suzuki-Miyaura cross-coupling reaction is discussed. It was shown that matching the bulk temperature of a thermal reference reaction with its parent illuminated reaction improves the comparability of both reactions. Furthermore, it was found that equating the temperature profile of the thermal control reaction with the temperature of its parent illuminated reaction yielded highly comparable reaction kinetics. This provides clear evidence for the predominant role of temperature on the reaction kinetics over possible heterocatalytic phenomena in this reaction. Variations in the amount of rate-determining reactant, amount of catalyst, and illumination intensities all result in the same observation: there is no distinct difference between the illuminated reactions and their respective thermal reference reactions. We therefore conclude that this reaction in particular is predominantly thermally driven.

Local temperatures directly at the surface of the nanoparticle can play a role in plasmon-assisted chemistry. The local temperatures of plasmonically excited nanoparticles are typically above the bulk reaction temperature. It is unlikely that such elevated local temperatures in this system are of any significance, since the reaction kinetics can already be ascribed to the observed bulk temperature effects. A hot filtration test was an effective way to remove the plasmonic nanoparticles from the reaction mixture, thereby removing the photocatalytic component, while maintaining all other physical parameters. This showed that the reaction was at least partially catalyzed by a secondary species, most likely in the form of leached Pd

© 2019 Wiley-VCH Verlag GmbH & Co. KGaA, Weinheim

nanoparticles or Pd ions. Additionally, it was shown that the reaction requires a temperature threshold of approximately 40 °C, which can explain the previously reported low conversion rates at low laser powers.

This research corroborates the hypothesis that the bulk temperature of the reaction and the leaching of catalytically active Pd from the catalyst plays a decisive role in the formation of the reaction product. We wish to stress that this insight is solely valid for the Suzuki-Miyaura cross-coupling of bromobenzene and *m*-tolylboronic acid, studied using the plasmonic Au@Pd catalyst and reaction conditions reported in this article. Future research will have to show how general these observations are for other chemical reactions. More effort should be invested in the internal stabilization of the catalyst in order to make the Au@Pd nanoparticle system suitable for any truly photocatalytic applications.

Experimental Section

Chemicals and Materials

Nanoseedz250 Au@Pd NRs were acquired from Nanoseedz Ltd (Hong Kong SAR, China) and used without purification. Bromobenzene (99%), *m*-tolylboronic acid (97%), sodium hydroxide (99.99%), hexadecyltrimethylammonium bromide (CTAB, $\geq$98%), 3-phenyltoluene (95%), biphenyl (99.5%), 3,3′-dimethylbiphenyl (99%), and hexadecane (99%) were acquired from Sigma Aldrich and were used as received. All reaction mixtures were prepared using ultrapure water.

Catalyst Characterization

The catalyst suspension was used as received. Au and Pd contents were determined with flame atomic absorption spectroscopy (AAS, Perkin Elmer 100 B), morphology and elemental topology were verified with transmission electron microscopy - energy-dispersive X-ray spectroscopy (TEM-EDX, JEOL ARM200F operated at 200 kV), and plasmon resonance was checked with UV-Vis spectroscopy (Hitachi U2001).

Catalyst Testing and Stability

A set of two reactions was simultaneously performed in airtight 1x1-cm quartz cuvettes: one under continuous 808-nm laser irradiation (R808$\pm$10-4WF-04LTR diode laser, Laser Components GmbH, Mönchengladbach, Germany) focused to a spot size of 3.33 mm and external power control using a programmable power supply (Keithley 2200–30-5 Tektronics, Beaverton, USA); the other in a dark, temperature-controlled stage (TC125, Quantum Northwest Inc, Liberty Lake, USA). The temperatures of both continuously stirred mixtures were monitored using two immersed thermocouples (735-2, Testo SA, Lenzkirch, Germany). The temperature of the parallel isothermal reaction was manually and iteratively adjusted to the temperature of the irradiated reaction to obtain two temperature plots with temporal differences of only a few °C. 50 μL aliquots were taken from the reaction mixture at designated times. The reaction components were extracted using diethyl ether (Biosolve, analytical grade) and subjected to GC analysis (Thermo Scientific Trace 1300, equipped with a Restek RTX200 column). Hexadecane was used as internal standard. Obtained peaks were automatically integrated using the Chromeleon software package (Thermo Scientific). A set of reactions was redone when a non-closed mass balance (90% > MB > 110%) was encountered. Sets of parallel experiments were performed using the laser in one set-up and the temperature-controlled reactor in the other. The temperature of the reaction mixture was continuously recorded, and the thermostat of the isothermal reaction was continuously set to this value. 50 μL aliquots were extracted at designated times and subjected to GC analysis. Again, two sets of two parallel experiments were performed, now with varying amounts of bromobenzene as rate-determining reactant,[18] and catalyst. The bromobenzene concentration in the first set of experiments was varied from 0.01 M to 0.04 M. The catalyst concentration in the second set was varied from 0.25x to 4x the Au concentration, compared to the fixed concentration of 26 μg of Au and 16 μg Pd in the other experiments. All other conditions were kept unchanged. The influence of Pd leaching from the particles is studied by performing a hot filtration test. The catalytic reaction at 1.5 W of laser power and the corresponding thermal reaction mixture are interrupted after 14 min, at which both reaction mixtures were immediately cooled in an ice-water bath to 0 °C. The reaction mixtures were subjected to centrifugation (4×15 min at 15,000×g) followed by extraction of the supernatant. The supernatants were subjected again to the same laser power and consecutive heating for another 40 min.

Acknowledgements

Analytische Laboratorien GmbH (Lindlar, Germany) is acknowledged for performing the AAS measurements. Eurofins Scientific (Eindhoven, the Netherlands) is acknowledged for performing the TEM-EDX imaging. The Netherlands Organisation for Scientific Research (NWO) is thanked for funding via a TA program (project number 731.013.201).

Conflict of Interest

The authors declare no conflict of interest.

Keywords: Plasmon-assisted chemistry · Suzuki-Miyaura cross-coupling reaction · Nanoplasmonics · Photocatalysis

[1] K. A. Willets, R. P. Van Duyne, *Annu. Rev. Phys. Chem.* **2007**, *58*, 267–297.
[2] a) T. V. Shahbazyan, *Phys. Rev. B* **2016**, *94*, 235431; b) G. Baffou, J. Polleux, H. Rigneault, S. Monneret, *J. Phys. Chem. C* **2014**, *118*, 4890–4898.
[3] J. R. Adleman, D. A. Boyd, D. G. Goodwin, D. Psaltis, *Nano Lett.* **2009**, *9*, 4417–4423.
[4] L. Zhou, C. Zhang, M. J. McClain, A. Manjavacas, C. M. Krauter, S. Tian, F. Berg, H. O. Everitt, E. A. Carter, P. Nordlander, N. J. Halas, *Nano Lett.* **2016**, *16*, 1478–1484.
[5] a) X. Zhang, X. Li, D. Zhang, N. Q. Su, W. Yang, H. O. Everitt, J. Liu, *Nat. Commun.* **2017**, *8*, 14542; b) X. Zhang, X. Li, M. E. Reish, D. Zhang, N. Q. Su, Y. Gutiérrez, F. Moreno, W. Yang, H. O. Everitt, J. Liu, *Nano Lett.* **2018**, *18*, 1714–1723; c) F. Sastre, A. V. Puga, L. Liu, A. Corma, H. García, *J. Am. Chem. Soc.* **2014**, *136*, 6798–6801; d) X. Meng, T. Wang, L. Liu, S. Ouyang, P. Li, H. Hu, T. Kako, H. Iwai, A. Tanaka, J. Ye, *Angew. Chem. Int. Ed.* **2014**, *53*, 11478–11482; *Angew. Chem.* **2014**, *126*, 11662–11666; e) F. Sastre, C. Versluis, N. Meulendijks, J. Rodríguez-Fernández, J. Sweelssen, K. Elen, M. K. Van Bael, T. den Hartog, M. A. Verheijen, P. Buskens, *ACS Omega* **2019**, *4*, 7369–7377.

© 2019 Wiley-VCH Verlag GmbH & Co. KGaA, Weinheim

[6] Z. Fang, Y.-R. Zhen, O. Neumann, A. Polman, F. J. García de Abajo, P. Nordlander, N. J. Halas, *Nano Lett.* **2013**, *13*, 1736–1742.
[7] a) L. Zhou, D. F. Swearer, C. Zhang, H. Robatjazi, H. Zhao, L. Henderson, L. Dong, P. Christopher, E. A. Carter, P. Nordlander, N. J. Halas, *Science* **2018**, *362*, 69; b) Y. Yu, V. Sundaresan, K. A. Willets, *J. Phys. Chem. C* **2018**, *122*, 5040–5048; c) R. M. Sarhan, W. Koopman, R. Schuetz, T. Schmid, F. Liebig, J. Koetz, M. Bargheer, *Sci. Rep.* **2019**, *9*, 3060.
[8] N. Miyaura, K. Yamada, A. Suzuki, *Tetrahedron Lett.* **1979**, *20*, 3437–3440.
[9] a) F. Kerins, D. F. O'Shea, *J. Org. Chem.* **2002**, *67*, 4968–4971; b) M. E. Trusova, M. Rodriguez-Zubiri, K. V. Kutonova, N. Jung, S. Bräse, F.-X. Felpin, P. S. Postnikov, *Org. Chem. Front.* **2018**, *5*, 41–45.
[10] a) A. F. Littke, C. Dai, G. C. Fu, *J. Am. Chem. Soc.* **2000**, *122*, 4020–4028; b) W.-Y. Siau, Y. Zhang, Y. Zhao, in *Stereoselective Alkene Synthesis* (Ed.: J. Wang), Springer, Berlin, Heidelberg, **2012**, pp. 33–58.
[11] H.-J. Lehmler, L. W. Robertson, *Chemosphere* **2001**, *45*, 137–143.
[12] a) Z. Jiao, Z. Zhai, X. Guo, X.-Y. Guo, *J. Phys. Chem. C* **2015**, *119*, 3238–3243; b) X.-H. Li, M. Baar, S. Blechert, M. Antonietti, *Sci. Rep.* **2013**, *3*, 1743.
[13] K. Mori, M. Kawashima, H. Yamashita, *Chem. Commun.* **2014**, *50*, 14501–14503.
[14] I. Sarhid, I. Abdellah, C. Martini, V. Huc, D. Dragoe, P. Beaunier, I. Lampre, H. Remita, *New J. Chem.* **2019**, *43*, 4349–4355.
[15] F. Wang, C. Li, H. Chen, R. Jiang, L.-D. Sun, Q. Li, J. Wang, J. C. Yu, C.-H. Yan, *J. Am. Chem. Soc.* **2013**, *135*, 5588–5601.
[16] a) C. Li, R. Sato, M. Kanehara, H. Zeng, Y. Bando, T. Teranishi, *Angew. Chem. Int. Ed.* **2009**, *48*, 6883–6887; *Angew. Chem.* **2009**, *121*, 7015–7019; b) J. M. Sanz, D. Ortiz, R. Alcaraz de la Osa, J. M. Saiz, F. González, A. S. Brown, M. Losurdo, H. O. Everitt, F. Moreno, *J. Phys. Chem. C* **2013**, *117*, 19606–19615.
[17] a) Y. Sang, H. Liu, A. Umar, *ChemCatChem* **2014**, *7*, 559–573; b) J. R. Cole, N. J. Halas, *Appl. Phys. Lett.* **2006**, *89*, 153120; c) E. K. Payne, K. L. Shuford, S. Park, G. C. Schatz, C. A. Mirkin, *J. Phys. Chem. B* **2006**, *110*, 2150–2154.
[18] G. B. Smith, G. C. Dezeny, D. L. Hughes, A. O. King, T. R. Verhoeven, *J. Org. Chem.* **1994**, *59*, 8151–8156.
[19] a) N. Ortiz, S. J. Hong, F. Fonseca, Y. Liu, G. Wang, *J. Phys. Chem. C* **2017**, *121*, 1876–1883; b) H. Jing, H. Wang, *CrystEngComm* **2014**, *16*, 9469–9477.
[20] a) W. Albrecht, J. E. S. van der Hoeven, T.-S. Deng, P. E. de Jongh, A. van Blaaderen, *Nanoscale* **2017**, *9*, 2845–2851; b) A. B. Taylor, A. M. Siddiquee, J. W. M. Chon, *ACS Nano* **2014**, *8*, 12071–12079.
[21] P.-P. Fang, A. Jutand, Z.-Q. Tian, C. Amatore, *Angew. Chem. Int. Ed.* **2011**, *50*, 12184–12188; *Angew. Chem.* **2011**, *123*, 12392–12396.

Manuscript received: June 24, 2019
Accepted manuscript online: August 9, 2019
Version of record online: September 18, 2019

© 2019 Wiley-VCH Verlag GmbH & Co. KGaA, Weinheim